

Article

Performance Comparison of Different Cathode Strategies on Air-Cathode Microbial Fuel Cells: Coal Fly Ash as a Cathode Catalyst

Asimina Tremouli ^{1,*}, Pavlos K. Pandis ¹, Theofilos Kamperidis ¹, Christos Argirusis ¹,
Vassilis N. Stathopoulos ² and Gerasimos Lyberatos ^{1,3}

¹ School of Chemical Engineering, National Technical University of Athens, 15780 Athens, Greece

² Laboratory of Chemistry and Materials Technology, Department of Agricultural Development, Agrofood and Management of Natural Resources, National and Kapodistrian University of Athens, Psachna Campus, 34400 Psachna, Greece

³ Institute of Chemical Engineering Sciences (ICE-HT), Stadiou Str., Platani, 26504 Patras, Greece

* Correspondence: atremouli@chemeng.ntua.gr

Abstract: The effect of different cathode strategies (mullite/MnO₂, Plexiglas/Gore-Tex/MnO₂, mullite/coal fly ash, mullite/biochar, mullite/activated carbon) on the performance of air-cathode microbial fuel cells (MFCs) was investigated. The highest maximum power output was observed using MnO₂ catalyst pasted on Gore-Tex cloth (7.7 mW/m³), yet the highest coulombic efficiencies (CEs) were achieved using MnO₂ (CE 23.5 ± 2.7%) and coal fly ash (CE 20 ± 3.3%) pasted on ceramic. The results showed that the utilization of coal fly ash and biochar as catalysts in MFC technology can be a sustainable and cost-effective solution.

Keywords: microbial fuel cell; fly ash; biochar; MnO₂; activated carbon; ceramic; mullite



Citation: Tremouli, A.; Pandis, P.K.; Kamperidis, T.; Argirusis, C.; Stathopoulos, V.N.; Lyberatos, G. Performance Comparison of Different Cathode Strategies on Air-Cathode Microbial Fuel Cells: Coal Fly Ash as a Cathode Catalyst. *Water* **2023**, *15*, 862. <https://doi.org/10.3390/w15050862>

Academic Editors: Silvia Fiore, Elia Judith Martínez Torres and Federico Aulenta

Received: 21 December 2022

Revised: 1 February 2023

Accepted: 21 February 2023

Published: 23 February 2023



Copyright: © 2023 by the authors. Licensee MDPI, Basel, Switzerland. This article is an open access article distributed under the terms and conditions of the Creative Commons Attribution (CC BY) license (<https://creativecommons.org/licenses/by/4.0/>).

1. Introduction

Over recent decades, microbial fuel cells (MFCs) have attracted research interest because of their unique feature of treating wastewater while producing electricity. Microbial fuel cells (MFCs) are systems in which microorganisms function as catalysts and convert the chemical energy contained in the chemical bonds of biomass and waste directly to electrical energy [1,2]. The direct power production during wastewater treatment using the MFC process could be a solution to current issues that conventional wastewater treatment practices face.

In particular, aerobically activated sludge requires large amounts of energy for aeration, recirculation and wastewater pumping. An MFC could be used in a treatment system as an alternative to an energy-demanding activated sludge system, resulting in net energy production rather than consumption. Moreover, the activated sludge process produces large amounts of sewage sludge, since it is an aerobic process, compared to use of anaerobic MFC technology, which generates only a small amount of microbial mass. Sludge handling drastically increases the operational and energy costs of typical wastewater treatment plants [3,4]. Currently, anaerobic digestion (AD) is widely applied as an alternative method for wastewater treatment since it saves energy sources and is highly effective in converting organic chemicals into methane (CH₄) gas. However, AD technology, unlike the MFC process, is not, in general, feasible when treating low-strength wastewater, such as municipal wastewater. Additionally, the use of AD as an electricity producing process is a two-step process (methane generation followed by burning in an internal combustion engine), in contrast to the MFC system, which produces electricity directly [5].

Although much effort has been applied towards the practical implementation of MFC technology in the field of wastewater treatment, there are still practical barriers to overcome

before utilization of these systems is possible. The main obstacles are the low power output obtained, due to high internal resistance and current instability, as well as the high costs of the materials [6]. In this context, the practical implementation of the technology can be achieved through an MFC system that has the appropriate design for scaling up and can be conveniently combined with existing wastewater treatment facilities, while ensuring high performance using cost-effective construction materials.

In this direction, several air-cathode, membrane-less, single-chamber configurations have been examined since these designs increase power production and reduce the capital cost of MFCs [7,8]. In such systems, various inexpensive and sustainable materials have been tested as separators and as cathode catalysts [9,10]. In this regard, ceramics are very promising materials to be used as separators in MFCs due to their wide availability, low cost, structural stability, durability and environmental friendliness when compared to other materials [11]. Several studies can be found in the literature using different types of ceramics as separators while treating wastewater [12–16]. In addition, in order to overcome the low performance of air-cathode systems because of the poor cathode oxygen reduction reaction (ORR) [17], the use of platinum has been widely examined [18]. However, since the use of Pt hinders the practical implementation of MFC technology due to its high cost and low availability, platinum cathode catalysts have been replaced by carbon-based, metal-free, transition-metal-oxide-based catalysts, as well as metal-nitrogen-carbon catalysts [19].

Beyond the cost-effectiveness of carbon metal-free catalysts, these materials have recently attracted significant attention because they do not suffer from crossover effects and have long-term operational stability [20]. In particular, activated carbon has a high specific surface area, rich porous structure, high mechanical strength and stable properties, as well as excellent acid/alkali resistance [21]. In the same context, biomass-derived black carbon (biochar) has recently attracted attention as an electrode material in MFC technology since it is a cost-effective and environmentally friendly material [22,23]. In addition, manganese dioxide is a transition metal oxide that has been extensively used as a cathode catalyst in MFC systems due to its environmentally friendly characteristics, good electrocatalytic activity and chemical stability [8,24,25].

Coal fly ash (CFA) is a solid waste that is produced by the combustion of coal in power plants. Nowadays, CFA is stored in landfills and ponds or is disposed of by simple stack. These methods are not environmentally friendly, since CFA contains contaminants, such as mercury, cadmium and arsenic, and, without proper management, these contaminants can pollute waterways, groundwater, drinking water, and the air [26]. However, CFA mainly consists of oxides, such as SiO_2 , Al_2O_3 , Fe_2O_3 , TiO_2 and CaO [27], and can be considered as a valuable raw material and source of transition metals. In this context, currently fly ash is reused in sectors such as cement, concrete, structural fill, soil stabilization and agriculture [27]. Considering that less than 30% of the total amount of fly ash generated is reused, other exploitation options for commercial applications need to be explored [27]. Only, recently, Jia et al., 2018 [28], suggested the exploitation of FA mixed with sewage sludge as the anode electrode in an MFC system, whereas Chen et al., 2022 used municipal solid waste incinerator bottom ash as an electrode plate in a dual chamber MFC since FA contains several different metals and metal oxides and can potentially be used as a cathode catalyst in an MFC unit [29].

In this study, we developed five different strategies to improve the cathode performance of a single-chamber, four-air cathode MFC (4ACMFC) seeking to use cost-effective and environmentally friendly materials [30]. Specifically, we manufactured five identical 4ACMFC systems using different cathode electrode assemblies. In particular, MnO_2 was used as a catalyst, while both Gore-Tex cloth and mullite were used as separators and cathode catalyst supports. In addition, activated carbon, biochar and CFA were placed on mullite tubes and their effectiveness as cathode catalysts was examined and compared. The performance of the 4ACMFCs was assessed in terms of organic matter (COD) removal and electricity production. Electrochemical characterization of the systems using impedance spectroscopy was also performed. The key novel contribution of the present work lies in

the fact that, for the first time, a four-air cathode, single-chamber microbial fuel cell, which was constructed using specific selection and combination of materials, was examined using the above cathode strategies, whereby, to the best of the authors' knowledge, CFA was applied for the first time on a ceramic and used as a cathode electrode in an MFC system.

2. Materials and Methods

2.1. MFC Construction

Five identical MFCs, but with different cathode assemblies, were constructed based on a 4ACMFC design [24,30–32]. The new units ($V = 659 \text{ cm}^3$) consisted of a single Ertalon[®] chamber, as shown in Figure 1c. The total height of each cell was 11.5 cm, whereas the “active height” (anode chamber) was 8 cm (Figure 1b). The internal diameter of each unit was 11 cm. One circular Ertalon[®] lid sealed the top of the anodic chamber. The lid was constructed to fit up to four tubes with an external diameter of 2 cm (Figure 1a). The tubes ran through the chamber and served as separators and as support for the cathode electrocatalyst. The new units were manufactured taking advantage of the positive aspects and avoiding the negative aspects of the 4ACMFC design [24,30] based on experience of its operation. Specifically, the new units have more flexibility and stability in their construction characteristics. In particular, the original 4ACMFC unit was made of Plexiglas [30,32], whereas, in the case of the new units used in this work, this material was replaced by Ertalon. The original 4ACMFC unit was constructed by joining a Plexiglas conical base and a circular lid to a cylinder, while the new units consisted of one cylinder with one top lid (Figure 1b). By making this modification, the design was made more compact and less sensitive to leakages. In addition, the cathode tubes which run through the cylinder had “plug and play” characteristics, which means they could be easily removed and replaced (Figure 1b,c). On the other hand, the cathode tubes of the 4ACMFC were silicon-glued and were removed with difficulty.

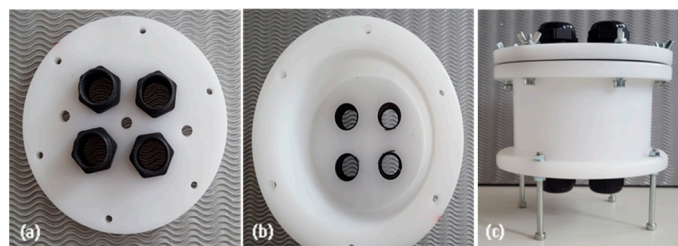


Figure 1. Photos of (a) the top lid, (b) the internal view and (c) the MFC units.

Graphite granules (type 00514, Le Carbone, Belgium), with diameters ranging between 1.5 and 5 mm, were used as the anodic biofilm support and conducting material, conveying electrons to a graphite rod (13 cm long by 7 mm diameter) inserted into the packed bed of granules with an active volume of 150 cm^3 . The cathode tubes were open to the atmosphere and no special aeration was employed.

2.2. Electrode Assembly Preparation

Four different ceramic cathode assemblies were prepared using MnO_2 (EMD Tosoh Hellas) (M-MnO_2), activated carbon (AC) (Sigma-Aldrich, CAS 7440-44-0), wood biochar (BC) (15–150 μm) and coal fly ash (CFA) (acquired from Megalopoli Power Plant in Arcadia, Greece) as cathode catalysts. Mullite, (Bonis S.A., Athens, Greece) (external diameter 25 mm, internal diameter 20 mm, porosity 18–20%), was used as the separator and catalyst support. In addition, Plexiglas tubes (2 cm diameter and 2 mm thickness) were used for the construction of one MFC unit (P-MnO_2). The tubes were uniformly perforated with circular holes (2 mm diameter) [9].

A prior mix containing 5 g of each of the above material/catalysts with 10 mL of graphite paint (HSF54–YSHIELD, Germany) was prepared and diluted in an EtOH/2-propanol 1:1 vol% of 20 mL. The slurry was sonicated for 30 min in order to be homogenized,

and then a paste was formed. The paste was brushed onto the inner surface of the ceramic tubes as reported elsewhere [10]. In the case of the Plexiglas tubes, the cloth was tightly bound on the outside wall of each perforated tube and the side covered with the MnO_2 coating was placed at the air-facing side. The final form of the ceramic cathodes is depicted in Figure 2.



Figure 2. Ceramic electrodes produced.

2.3. Operation

The five units were operated under identical conditions in order to compare the performance of the different cathode assemblies. The enrichment and adaptation of the electrochemically active bacteria were performed in batch mode, under a fixed external load of 100Ω for each cell. During inoculation, 10% *v/v* of anaerobic sludge collected from the Lykovrysi Wastewater Treatment Plant of Athens, Greece, was used as the inoculum, whereas glucose-based synthetic wastewater (1 gCOD/L) was used as the feed [9]. Following the enrichment of cells, only glucose-based synthetic medium (1 gCOD/L) was used.

2.4. Analytical Methods

The performance of the units was evaluated in terms of COD removal efficiency, and CE and volumetric power density, normalized for the anodic liquid volume (150 cm^3). The COD removal efficiency and the CE were calculated as described by Logan et al. [33]. The voltage of the units was recorded at 2 min intervals by a Keysight LXI Data Acquisition system. The measurements of pH and conductivity were conducted using digital instruments WTW INOLAB PH720 and WTW INOLAB, respectively. The soluble COD was measured according to standard methods [34].

All electrochemical experiments were carried out using a potentiostat–galvanostat (PGSTAT128N—AUTOLAB) with a two-electrode set-up. Linear sweep voltammetry (LSV) was conducted from open current voltage (OCV) to short circuit, with a step of 0.005 mV/s , in order to estimate the polarization curves of the cell. In addition, electrochemical impedance spectroscopy (EIS) was performed in the whole cell in order to calculate the internal resistances and further justify the results. A two-electrode setup was applied for the above measurements. The working electrode of the potentiostat was connected to the anode side, whilst the reference and counter electrode were connected to the four cathodic electrodes. The data were collected over the frequency range of $100 \text{ kHz}–1 \text{ mHz}$, applying a stimulus of a 10 mV amplitude regarding the sinusoidal signal. The electrical equivalent circuit used to simulate the EIS curves was the same as reported elsewhere [10] and is depicted as an inset in the Nyquist Diagram in Section 3.3.

3. Results and Discussion

3.1. MFC Operation

In order to assess the different cathode strategies, following the acclimation of the units, the MFCs operated in batch mode for approximately 480 h. Figure 3 demonstrates the current output profiles produced from the five units, while the CE and COD removal efficiency from MFCs equipped with the different cathode materials (P- MnO_2 , M- MnO_2 , CFA, BC, AC) are summarized in Figures 4 and 5.

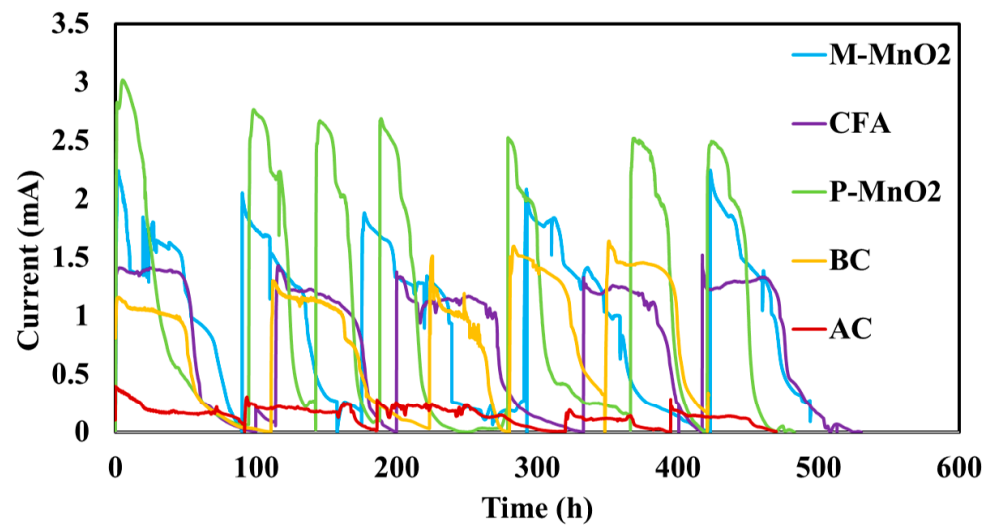


Figure 3. Current output during consecutive batch experiments of the five units with the different cathode assemblies (P-MnO₂, M-MnO₂, CFA, BC, AC) versus time.

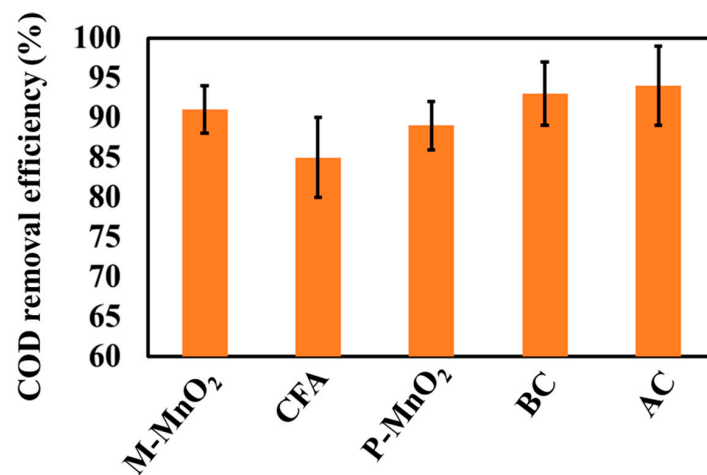


Figure 4. Average COD removal efficiency values with deviations of the five units with the different cathode assemblies (P-MnO₂, M-MnO₂, CFA, BC, AC) versus time.

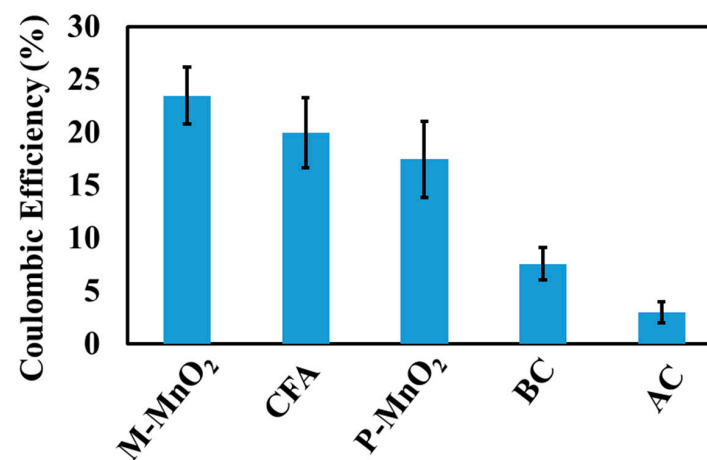


Figure 5. Average CE efficiency values with deviations of the five units with the different cathode assemblies (P-MnO₂, M-MnO₂, CFA, BC, AC) versus time.

The results obtained showed that the P-MnO₂ assembly achieved the highest I_{\max} of 2.7 ± 0.2 mA, followed by M-MnO₂ with 2.1 ± 0.1 mA, BC with 1.5 ± 0.1 mA, CFA with 1.5 ± 0.2 mA and AC with 0.3 ± 0.1 mA. Although the maximum current output was obtained from the P-MnO₂ assembly, the M-MnO₂ unit outperformed in terms of coulombic efficiency (CE), with the second highest CE value achieved from the CFA unit. In particular, the CE values were $23.5 \pm 2.7\%$, $20 \pm 3.3\%$, $17.5 \pm 3.6\%$, $7.6 \pm 1.5\%$, $3 \pm 1\%$, for the M-MnO₂, CFA, P-MnO₂, BC and AC units, respectively. Regardless of the performance of the MFCs in terms of current output and CE, all the systems successfully removed the organic substrate of the synthetic wastewater. Specifically, the following COD removal efficiencies were obtained: $94 \pm 5\%$ (AC), $93 \pm 4\%$ (BC), $91 \pm 3\%$ (M-MnO₂), $89 \pm 3\%$ (P-MnO₂), $85 \pm 5\%$ (CFA). Despite the different cathode assemblies used, the high COD removal efficiency values confirmed the presence of non-electrogenic bacteria in the anode chamber, which also consume organic matter of the wastewater along with the electrogenic bacteria [35].

3.2. Effect of the Different Cathode Strategies on the Polarization Performance of the MFC Units

Figure 6a,b show the dependence of the MFC voltage, V , and the produced power volumetric density, P , on the current density passing through the units with the different cathode assemblies. As shown in Figure 6a, the open circuit voltage (OCV) was ~ 0.44 V for the assemblies M-MnO₂, CFA, BC and AC, whereas, the OCV value for the P-MnO₂ configuration was 0.52 V. The P-MnO₂ configuration achieved the highest maximum power volumetric density at 7.7 mW/m³, followed by M-MnO₂ with 5.5 mW/m³, CFA with 2.9 mW/m³, BC with 1.9 mW/m³ and AC with 1.1 mW/m³ (Figure 6b).

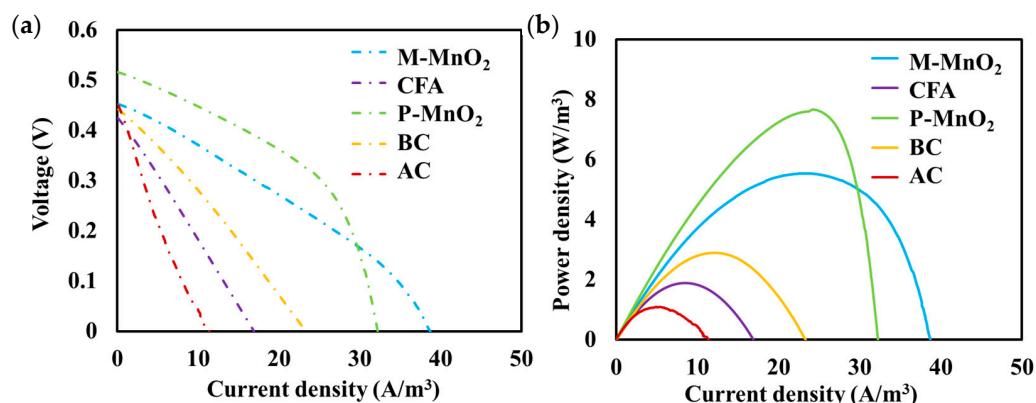


Figure 6. MFC voltage U_{cell} (a) and power density (b) versus current density for the different cathode strategies (P-MnO₂, M-MnO₂, CFA, BC, AC).

In addition, the internal resistances (R_{in}) of the CFA, BC and AC assemblies, as determined by the power density peak method, were 133Ω , 177Ω and 298Ω , respectively. Moreover, the almost constant slope of the polarization curves of these units (Figure 6a) indicated the very significant contribution of ohmic losses (ohmic overpotential) for the CFA, BC and AC assemblies. The internal resistance for the MnO₂ catalyst was lower when compared to the other catalysts, regardless of the structural support used (R_{in} was 64Ω and 70Ω for P-MnO₂ and M-MnO₂, respectively). On the other hand, when an MnO₂ catalyst was used, in addition to the ohmic losses that occurred, a rapid voltage drop was also observed at high current densities, indicating mass transport limitations (Figure 6a).

3.3. Electrochemical Impedance Spectroscopy Characterization

Considering the results on the EIS of the cells, Figure 7 depicts the Nyquist Diagrams of the cells.

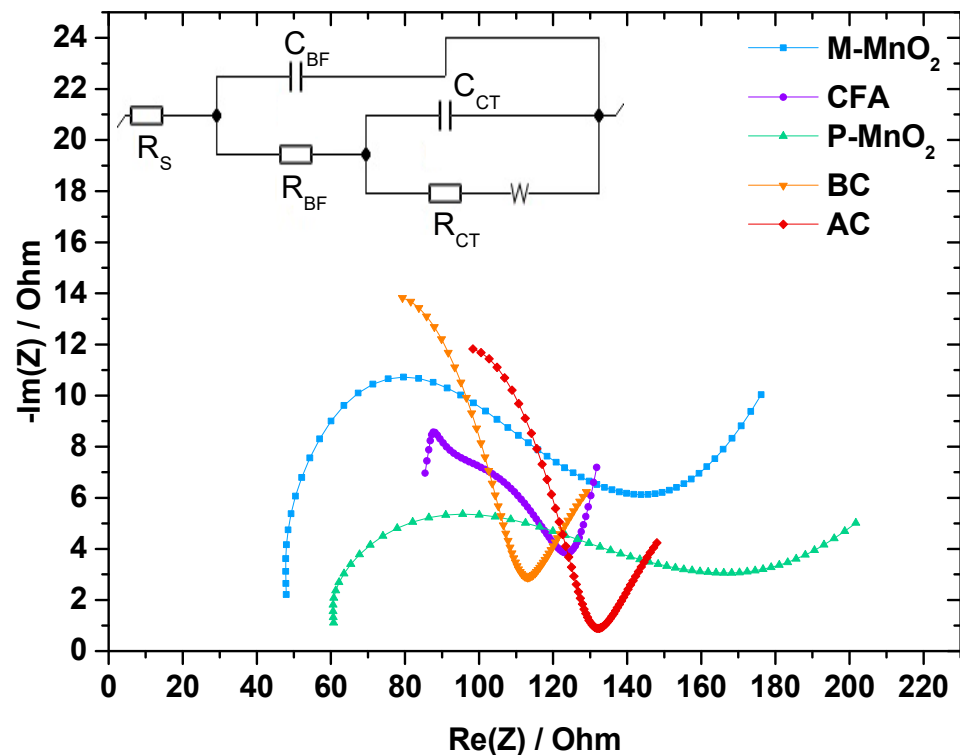


Figure 7. Nyquist (Bode-Bode) plots from EIS measurements.

In Figure 7, Nyquist plots for all cell strategies are depicted. All contain one arc and Warburg diffusion. This implies that all resistances in the cells were caused by the resistance of biofilm and charge transfer resistances from the electrodes.

The numerical results were calculated through Z-fit analysis and are shown in Table 1. Prior to any comment on these values, the internal resistances were verified through EIS and had the same results as the values of internal resistances from Jacobi's law. There were obvious differences between the values of R_S , R_{BF} and R_{CT} between all the proposed cell modifications. The values C_{BF} and C_{CT} refer to the capacitance of the biofilm and the capacitance of charge transfer of the electrodes, respectively. The C_{BF} value corresponds to the accumulation rate of the biofilm in the anode side, whilst C_{CT} refers to the accumulation of the responsible moieties for the charge transfer [35–40]. Between M-MnO₂ and P-MnO₂, there were certain differences in the R_{CT} value. The higher value in the case of P-MnO₂ indicated that the electrodes increased the charge transfer resistance three times in relation to the M-MnO₂. In addition, the C_{CT} value was significantly higher in the case of P-MnO₂, and this is attributed to mass transport limitations, as reported also in Figure 6a. The different cathode assemblies also contributed to different values in R_{CT} for the rest cell strategies (CFA, BC and AC). In the case of AC, the R_{CT} value was significantly higher and, having a low value of C_{CT} , explained the poor electrical output of the cell. BC seemed to have operated and produced lower power output in relation to the P-MnO₂, M-MnO₂ and CFA strategies, and this was supported by the same trend in all the resistance values. The coulombic efficiency presented mostly the same trend as C_{CT} for the different cell modes. The high values of C_{CT} observed imply a larger accumulation of the species responsible for the enhancement of R_{CT} values. In addition, the high R_{CT} values imply reduction in the power output values and coulombic efficiency of the cells.

Table 1. Fitting parameters from EIS measurements.

Fitted Parameters	M-MnO ₂	CFA	P-MnO ₂	BC	AC
R _S (Ω)	32	81	31	75	90
R _{BF} (Ω)	36	35	35	39	114
R _{CT} (Ω)	2	17	8	60	75
CBF (F)	3 × 10 ⁻³	2 × 10 ⁻⁷	5 × 10 ⁻³	2 × 10 ⁻³	2 × 10 ⁻¹³
CCT (F)	9 × 10 ⁻⁷	9 × 10 ⁻³	0.7 × 10 ⁻⁴	5 × 10 ⁻³	1 × 10 ⁻³
R _{INT} (Ω) *	70	133	68	174	279

Note: * R_{INT} is the sum of all internal resistances.

4. Conclusions

The operation of five different MFC cathode assemblies was assessed and compared in terms of organic matter removal and electricity generation. Although the wastewater treatment was satisfactory for all cases (COD removal efficiency ≥ 85%), in terms of power generation, the MnO₂ catalyst outperformed coal fly ash (2.9 mW/m³), biochar (1.9 mW/m³) and activated carbon (1.1 mW/m³). In particular, the P-MnO₂ configuration achieved the highest maximum power volumetric density (7.7 mW/m³) in comparison to M-MnO₂ (5.5 mW/m³). Impedance experiments undertaken supported the results from the LSV curves and provided an explanation of the mass transport limitation of the cells. Although the MnO₂ configurations obtained the best performance, the results indicated that the exploitation of coal fly ash and biochar as cathode catalysts in MFC technology is promising, but more research is needed in order to further enhance their performance.

Author Contributions: Conceptualization, A.T. and G.L.; data curation, A.T., T.K. and P.K.P.; formal analysis, A.T., P.K.P. and T.K.; funding acquisition, A.T.; investigation, A.T., T.K. and P.K.P.; methodology, A.T., T.K. and P.K.P.; project administration, A.T.; resources, A.T., C.A., V.N.S. and G.L.; supervision, C.A., V.N.S. and G.L.; validation, A.T., P.K.P. and T.K.; visualization, A.T., T.K. and P.K.P.; writing—original draft, A.T., P.K.P. and T.K.; writing—review and editing, A.T., P.K.P. and T.K. All authors have read and agreed to the published version of the manuscript.

Funding: This project has received funding from the Hellenic Foundation for Research and Innovation (HFRI) and the General Secretariat for Research and Technology (GSRT), under grant agreement No [862].

Data Availability Statement: The datasets generated and analyzed during the current study are available from the corresponding author on reasonable request.

Conflicts of Interest: The authors declare no conflict of interest.

References

- Bennetto, H.P. Electricity generation by microorganisms. *Biotechnol. Educ.* **1990**, *1*, 163–168.
- Pant, D.; Van Bogaert, G.; Diels, L.; Vanbroekhoven, K. A review of the substrates used in microbial fuel cells (MFCs) for sustainable energy production. *Bioresour. Technol.* **2010**, *101*, 1533–1543. [[CrossRef](#)] [[PubMed](#)]
- Rabaey, K.; Lissens, G.; Verstraete, W. Microbial fuel cells: Performances and perspectives. In *Biofuels for Fuel Cells: Renewable Energy from Biomass Fermentation*, 1st ed.; Piet, L., Peter, W., Marianne, H., Angelo, M., Eds.; IWA Publishing: London, UK, 2005; pp. 377–399.
- Logan, B.E. *Microbial Fuel Cells*; John Wiley & Sons: Hoboken, NJ, USA, 2008. [[CrossRef](#)]
- Lefebvre, O.; Uzabiaga, A.; Chang, I.S.; Kim, B.-H.; Ng, H.Y. Microbial fuel cells for energy self-sufficient domestic wastewater treatment—A review and discussion from energetic consideration. *Appl. Microbiol. Biotechnol.* **2010**, *89*, 259–270. [[CrossRef](#)] [[PubMed](#)]
- Do, M.; Ngo, H.; Guo, W.; Liu, Y.; Chang, S.; Nguyen, D.; Nghiem, L.; Ni, B. Challenges in the application of microbial fuel cells to wastewater treatment and energy production: A mini review. *Sci. Total. Environ.* **2018**, *639*, 910–920. [[CrossRef](#)] [[PubMed](#)]
- Tremouli, A.; Kamperidis, T.; Lyberatos, G. Comparative Study of Different Operation Modes of Microbial Fuel Cells Treating Food Residue Biomass. *Molecules* **2021**, *26*, 3987. [[CrossRef](#)] [[PubMed](#)]
- Tremouli, A.; Kamperidis, T.; Pandis, P.K.; Argirusis, C.; Lyberatos, G. Exploitation of Digestate from Thermophilic and Mesophilic Anaerobic Digesters Fed with Fermentable Food Waste Using the MFC Technology. *Waste Biomass Valorization* **2021**, *12*, 5361–5370. [[CrossRef](#)]
- Kamperidis, T.; Pandis, P.K.; Argirusis, C.; Lyberatos, G.; Tremouli, A. Effect of Food Waste Condensate Concentration on the Performance of Microbial Fuel Cells with Different Cathode Assemblies. *Sustainability* **2022**, *14*, 2625. [[CrossRef](#)]

10. Pandis, P.K.; Kamperidis, T.; Bariamis, K.; Vlachos, I.; Argirusis, C.; Stathopoulos, V.N.; Lyberatos, G.; Tremouli, A. Comparative Study of Different Production Methods of Activated Carbon Cathodic Electrodes in Single Chamber MFC Treating Municipal Landfill Leachate. *Appl. Sci.* **2022**, *12*, 2991. [CrossRef]
11. James, A. Ceramic-microbial fuel cell (C-MFC) for waste water treatment: A mini review. *Environ. Res.* **2022**, *210*, 112963. [CrossRef]
12. Jeong, C.M.; Choi, J.D.R.; Ahn, Y.; Chang, H.N. Removal of volatile fatty acids (VFA) by microbial fuel cell with aluminum electrode and microbial community identification with 16S rRNA sequence. *Korean J. Chem. Eng.* **2008**, *25*, 535–541. [CrossRef]
13. Merino-Jimenez, I.; Obata, O.; Pasternak, G.; Gajda, I.; Greenman, J.; Ieropoulos, I. Effect of microbial fuel cell operation time on the disinfection efficacy of electrochemically synthesised catholyte from urine. *Process. Biochem.* **2020**, *101*, 294–303. [CrossRef] [PubMed]
14. Yousefi, V.; Mohebbi-Kalhari, D.; Samimi, A. Start-up investigation of the self-assembled chitosan/montmorillonite nanocomposite over the ceramic support as a low-cost membrane for microbial fuel cell application. *Int. J. Hydrogen Energy* **2019**, *45*, 4804–4820. [CrossRef]
15. Tremouli, A.; Greenman, J.; Ieropoulos, I. Investigation of ceramic MFC stacks for urine energy extraction. *Bioelectrochemistry* **2018**, *123*, 19–25. [CrossRef] [PubMed]
16. Tremouli, A.; Greenman, J.; Ieropoulos, I. Effect of simple interventions on the performance of a miniature MFC fed with fresh urine. *Int. J. Hydrogen Energy* **2021**, *46*, 33594–33600. [CrossRef] [PubMed]
17. Wang, Z.; Mahadevan, G.D.; Wu, Y.; Zhao, F. Progress of air-breathing cathode in microbial fuel cells. *J. Power Sources* **2017**, *356*, 245–255. [CrossRef]
18. Santoro, C.; Kodali, M.; Herrera, S.; Serov, A.; Ieropoulos, I.; Atanassov, P. Power generation in microbial fuel cells using platinum group metal-free cathode catalyst: Effect of the catalyst loading on performance and costs. *J. Power Sources* **2017**, *378*, 169–175. [CrossRef]
19. Freitas, W.D.S.; Gemma, D.; Mecheri, B.; D’Epifanio, A. Air-breathing cathodes for microbial fuel cells based on iron-nitrogen-carbon electrocatalysts. *Bioelectrochemistry* **2022**, *146*, 108103. [CrossRef]
20. Yuan, Y.; Yuan, T.; Wang, D.; Tang, J.; Zhou, S. Sewage sludge biochar as an efficient catalyst for oxygen reduction reaction in a microbial fuel cell. *Bioresour. Technol.* **2013**, *144*, 115–120. [CrossRef]
21. Zhang, Q.; Liu, L. A microbial fuel cell system with manganese dioxide/titanium dioxide/graphitic carbon nitride coated granular activated carbon cathode successfully treated organic acids industrial wastewater with residual nitric acid. *Bioresour. Technol.* **2020**, *304*, 122992. [CrossRef]
22. Huggins, T.; Wang, H.; Kearns, J.; Jenkins, P.; Ren, Z.J. Biochar as a sustainable electrode material for electricity production in microbial fuel cells. *Bioresour. Technol.* **2014**, *157*, 114–119. [CrossRef]
23. Chang, H.-C.; Gustave, W.; Yuan, Z.-F.; Xiao, Y.; Chen, Z. One-step fabrication of binder-free air cathode for microbial fuel cells by using balsa wood biochar. *Environ. Technol. Innov.* **2020**, *18*, 100615. [CrossRef]
24. Tremouli, A.; Pandis, P.K.; Kamperidis, T.; Stathopoulos, V.N.; Argirusis, C.; Lyberatos, G. Performance assessment of a four-air cathode membraneless microbial fuel cell stack for wastewater treatment and energy extraction. *E3S Web Conf.* **2019**, *116*, 00093. [CrossRef]
25. Liu, Y.; Guo, S.; Wang, J.; Li, C. Fundamental development and research of cathodic compartment in microbial fuel cells: A review. *J. Environ. Chem. Eng.* **2022**, *10*, 107918. [CrossRef]
26. Coal Ash Basics | US EPA. Available online: <https://www.epa.gov/coalash/coal-ash-basics#04> (accessed on 4 December 2022).
27. Jayaranjan, M.L.D.; van Hullebusch, E.D.; Annachhatre, A.P. Reuse options for coal fired power plant bottom ash and fly ash. *Rev. Environ. Sci. Biotechnol.* **2014**, *13*, 467–486. [CrossRef]
28. Jia, Y.; Feng, H.; Shen, D.; Zhou, Y.; Chen, T.; Wang, M.; Chen, W.; Ge, Z.; Huang, L.; Zheng, S. High-performance microbial fuel cell anodes obtained from sewage sludge mixed with fly ash. *J. Hazard. Mater.* **2018**, *354*, 27–32. [CrossRef]
29. Chen, C.-K.; Pai, T.-Y.; Lin, K.-L.; Ganesan, S.; Ponnusamy, V.K.; Lo, F.-C.; Chiu, H.-Y.; Banks, C.J.; Lo, H.-M. Electricity production from municipal solid waste using microbial fuel cells with municipal solid waste incinerator bottom ash as electrode plate. *Bioresour. Technol. Rep.* **2022**, *19*, 101210. [CrossRef]
30. Tremouli, A.; Intzes, A.; Intzes, P.; Bebelis, S.; Lyberatos, G. Effect of periodic complete anolyte replacement on the long term performance of a four air cathodes single chamber microbial fuel cell. *J. Appl. Electrochem.* **2015**, *45*, 755–763. [CrossRef]
31. Tremouli, A.; Pandis, P.K.; Karydogiannis, I.; Stathopoulos, V.N.; Argirusis, C.; Lyberatos, G. Operation and Electro(chemical) characterization of a microbial fuel cell stack fed with fermentable household waste extract. *Glob. NEST J.* **2019**, *21*, 253–257. [CrossRef]
32. Tremouli, A.; Martinos, M.; Bebelis, S.; Lyberatos, G. Performance assessment of a four-air cathode single-chamber microbial fuel cell under conditions of synthetic and municipal wastewater treatments. *J. Appl. Electrochem.* **2016**, *46*, 515–525. [CrossRef]
33. Cheng, S.; Logan, B.E. Increasing power generation for scaling up single-chamber air cathode microbial fuel cells. *Bioresour. Technol.* **2011**, *102*, 4468–4473. [CrossRef] [PubMed]
34. APHA/AWWA/WEF. *Standard Methods for the Examination of Water and Wastewater*, 22nd ed.; American Public Health Association (APHA): Washington, DC, USA, 2012; ISBN 9780875532356.
35. He, Z.; Minteer, S.D.; Angenent, L.T. Electricity Generation from Artificial Wastewater Using an Upflow Microbial Fuel Cell. *Environ. Sci. Technol.* **2005**, *39*, 5262–5267. [CrossRef] [PubMed]

36. Manohar, A.K.; Mansfeld, F. The internal resistance of a microbial fuel cell and its dependence on cell design and operating conditions. *Electrochim. Acta* **2008**, *54*, 1664–1670. [[CrossRef](#)]
37. Hidalgo, D.; Sacco, A.; Hernández, S.; Tommasi, T. Electrochemical and impedance characterization of Microbial Fuel Cells based on 2D and 3D anodic electrodes working with seawater microorganisms under continuous operation. *Bioresour. Technol.* **2015**, *195*, 139–146. [[CrossRef](#)] [[PubMed](#)]
38. Dominguez-Benetton, X.; Seveda, S.; Vanbroekhoven, K.; Pant, D. The accurate use of impedance analysis for the study of microbial electrochemical systems. *Chem. Soc. Rev.* **2012**, *41*, 7228–7246. [[CrossRef](#)] [[PubMed](#)]
39. Sekar, N.; Ramasamy, R.P. Electrochemical Impedance Spectroscopy for Microbial Fuel Cell Characterization. *J. Microb. Biochem. Technol.* **2013**, *6.2*, 1–14. [[CrossRef](#)]
40. Martin, E.; Savadogo, O.; Guiot, S.R.; Tartakovsky, B. Electrochemical characterization of anodic biofilm development in a microbial fuel cell. *J. Appl. Electrochem.* **2013**, *43*, 533–540. [[CrossRef](#)]

Disclaimer/Publisher’s Note: The statements, opinions and data contained in all publications are solely those of the individual author(s) and contributor(s) and not of MDPI and/or the editor(s). MDPI and/or the editor(s) disclaim responsibility for any injury to people or property resulting from any ideas, methods, instructions or products referred to in the content.